Human Pancreatic Lipase: An Exposed Hydrophobic Loop from the C-terminal Domain May Contribute to Interfacial Binding

Sofiane Bezzine, Frédéric Carrière, Josiane De Caro, Robert Verger, and Alain De Caro*

Unité Propre de Recherche 9025 de l'Institut Fédératif de Recherche 1, Laboratoire de Lipolyse Enzymatique du CNRS, 31, Chemin Joseph-Aiguier, 13402 Marseille Cedex 20, France

Received December 22, 1997; Revised Manuscript Received June 18, 1998

ABSTRACT: Epitope mapping was performed using four anti-HPL monoclonal antibodies (mAb's 81−23, 146−40, 315−25, and 320−24) directed against human pancreatic lipase (HPL). Three HPL mutants produced in insect cells were tested for this purpose: (i) N−HPL, which consists of only the N-terminal domain of HPL, (ii) HPL(-lid), in which a short loop consisting of 5 amino acid residues replaces the full-length 23-residue lid domain present in HPL, and (iii) N-GPLRP2/C−HPL chimera, a chimeric mutant consisting of the N-terminal domain of the guinea pig pancreatic lipase related protein 2 (GPLRP2) fused to the C-terminal domain of HPL. The C-terminal domain of HPL (C−HPL) was prepared in a pure form after performing chymotryptic digestion of HPL. The mAb 146−40 recognizes HPL, HPL(-lid), and N−HPL but not GPLRP2, N-GPLRP2/C−HPL chimera, or the C−HPL. The antibody mAb 146−40 therefore specifically recognizes the N-terminal domain of HPL, and the epitope recognized does not include the amphiphilic lid. On the other hand, mAb's 81−23, 315−25, and 320−24 react specifically to the C-terminal domain of HPL, since they recognize HPL, HPL(-lid), the N-GPLRP2/C−HPL chimera, and the C−HPL but not N−HPL or GPLRP2. It was further established that these three mAb's recognize the same conformational epitope, the structure of which is stabilized by the N-terminal domain in the presence of SDS at concentrations greater than its critical micellar concentration. This conformational epitope was found to be located in the vicinity of Met 397 and Arg 414. These two residues delineate a highly exposed peptide stretch extending from the HPL C-terminal domain, which includes a hydrophobic surface loop ($\beta 5'$). Kinetic studies on the HPL/mAb's complexes showed that the lipase activity was much lower in these complexes than in HPL. The results of the present study suggest for the first time that the $\beta 5'$ loop from the C-terminal domain may be involved in the interaction of HPL with a lipid/water interface.

Pancreatic lipase (triacylglycerol hydrolase, EC 3.1.1.3) catalyzes the intraduodenal conversion of triglycerides into diglycerides and subsequently into monoglycerides and free fatty acids (*1*). In 1981, the first amino acid sequence of porcine pancreatic lipase was published (*2*). Over the past few years, the amino acid sequences of other pancreatic lipases have been deduced from the corresponding cDNA in the case of several species, including humans (*3*, *4*), dogs (*5*), guinea pigs (*6*, *7*), rats (*8*, *9*), coypus (*10*, *11*), and rabbits (*12*). On the basis of primary structure comparisons, the pancreatic lipase family can be subdivided into three subgroups: (i) classical pancreatic lipases, (ii) pancreatic lipase-related protein 1 (PLRP1), and (iii) pancreatic lipase-related protein 2 (PLRP2) (*4*, *10*). It has been established that in the guinea pig (*6*), the coypu (*10*), and the rat (*13*), PLRP2 displays different kinetic properties from those of the classical lipases.

The resolution of the three-dimensional structure of classical human pancreatic lipase (HPL) (*14*) has shown that the single polypeptide chain (449 amino acids) is folded into two domains: a large N-terminal domain (residues 1−335), which shows a typical α/β hydrolase fold (*15*), and a C-terminal domain (residues 336−449), which is of the β-sandwich type (*14*). The serine 152, which is part of the Ser152-Asp167-His263 triad, is the nucleophilic residue involved in the catalysis: it is located in the N-terminal domain. A surface loop (Cys 237-Cys 261), the so-called lid or flap, prevents the access of the substrate to the active site in its closed conformation. HPL requires a small protein cofactor, colipase, for the enzyme to be able to bind to the bile salt-covered water/triglyceride interface. Colipase binds to the C-terminal domain of HPL (*16*), but it also interacts with the lid, once the latter has popped up after the cocrystallization occurring in the presence of mixed micelles (*17*). Colipase is a three-finger-shaped amphiphilic protein which facilitates the anchoring of HPL at the interface by exposing a large hydrophobic plateau consisting mainly of two surface loops (lid and $\beta 9$ loop) and the hydrophobic tips of the colipase fingers.

In the guinea pig, GPLRP2 is expressed by the exocrine pancreas in comparable amounts to the classical lipase (GPL) (*7*). On the basis of amino acid sequence comparisons between HPL, GPL, and GPLRP2, it appeared that the N-terminal domain (catalytic domain) is more highly conserved (67.8%) than the C-terminal domain (48.7%) (*7*). The

* To whom correspondence should be sent. Tel: 33−491 164 488. Fax: 33−491 715 857.

S0006-2960(97)03136-X CCC: $15.00
Published on Web 08/07/1998

"atypical" kinetic properties of GPLRP2, that is, a high phospholipase activity and the absence of interfacial activation, were initially attributed to the presence of a mini-lid consisting of 5 residues (*6*) replacing the full-length 23-residue lid present in HPL. The fact that the substrate had free access to the active site of GPLRP2 was confirmed when the 3-D structure of the N-GPLRP2/C−HPL chimera, a chimera mutant consisting of the catalytic N-terminal domain of GPLRP2 and the C-terminal domain of HPL, was elucidated (*18*). Chimeric mutants between HPL and GPLRP2 were recently produced by performing domain exchanges in order to investigate the structure−function relationships of pancreatic lipases (*19*).

Monoclonal antibodies (mAb's) are useful tools for mapping structural domains and for probing the functional features of multidomain enzymes such as lipases. Four anti-HPL mAb's (81−23, 146−40, 315−25, and 320−24) have been produced (*20*) at our laboratory and used to carry out epitope mapping on HPL. Four peptides obtained by performing limited chymotryptic cleavage were characterized by Western blotting and N-terminal amino acid sequence analysis. On the basis of the competitive binding observed between mAb's or Fab fragments with HPL, it was concluded (*20*) that mAb's 81−23, 315−25, and 320−24 recognize overlapping epitopes from the hinge region located between the N- and C-terminal domains of HPL.

In the present study, we checked the previous pancreatic lipase epitope mapping data using pancreatic lipase mutants and the previously described mAb's. The three mAb's 81−23, 315−25, and 320−24 did in fact all recognize the same conformational epitope located within the C-terminal domain of HPL. The kinetic properties of HPL/mAb complexes were further studied, and the role of the C-terminal domain in the interfacial binding of pancreatic lipase was established.

MATERIALS AND METHODS

DNA Manipulations. All the DNA manipulations were performed using standard methods (*21*). Restriction enzymes and T4 DNA ligase were purchased from New England Biolabs. DNA fragments were purified from agarose gel using the Gene Clean kit (Bio 101, Inc.). Sequencing was performed with the chain termination reaction method using the Sequenase Version 2.0 DNA Sequencing Kit (Amersham Life Science).

Construction of the DNA Encoding the N−HPL Mutant. Starting with HPL full-length cDNA (*22*), which served as the template, the N−HPL mutant was obtained by performing PCR using the following forward and reverse primers, both including a *Hin*dIII restriction site (underlined):

Primer 1, 5′-CCC AAG CTT GCT CGG CAT GCT CCC GCT CTG G-3′

Primer 2, 5′-GGG AAG CTT CTA TTA AAA ATT ACT GGC ATC ACC-3′

Primer 1 anneals with the HPL signal sequence encoding the peptide Met-Leu-Pro-Leu-Trp. Primer 2 includes a stop codon and anneals with an internal part of HPL cDNA encoding the last five amino acid residues of the HPL N-terminal domain (Gly-Asp-Ala-Ser-Phe335). The PCR reaction was carried out using pfu polymerase (Stratagene, la Jolla, CA) for 30 cycles with durations of 1 min at 94 °C, 2 min at 50 °C, and 3 min at 72 °C. The PCR product was cloned into the *Hin*dIII site of the pIC19R vector (*23*) and sequenced in order to check that no random mutation had been introduced by the PCR. Once the correct orientation of N−HPL DNA had been checked, it was further subcloned into the *Eco*RI/*Bgl*II sites of the pVL1393 baculovirus transfer vector (Invitrogen, San Diego, CA).

Obtaining the Recombinant Baculovirus Expressing N−HPL. Spodoptera frugiperda insect cells (Sf9) were grown in vitro in TNM-FH medium (Sigma) supplemented with 10% of fetal calf serum, at 27 °C. They were cotransfected as described in the BaculoGold transfection Kit manual (Pharmingen), using 0.5 μg of linearized viral DNA (AcMNPV) containing a lethal deletion and 2 μg of transfer vector mixed with liposomes. The lethal deletion can be restored by genetic recombination between the viral and transfer vector DNAs, and only recombinant viruses were therefore viable and able to replicate. Seven days after the cotransfection, 0.5 mL of the medium containing the recombinant virus was used to infect a fresh monolayer of Sf9 cells (10^7 cells in 10 mL of serum-free medium (Sf900) (GibcoBRL)) in order to check the expression of the recombinant protein and to determine the time course of the expression of N−HPL after cell infection.

Analysis of the Recombinant Virus. PCR amplification was performed in order to identify the recombinant virus and to check the length of the DNA insert within the polyhedrin gene of the baculovirus. Amplification was performed for 30 cycles at 95 °C for 1 min, at 55 °C for 2 min, and at 72 °C for 3 min. The forward (5′-TTTACT-GTTTTCGTAACAGTTTTG-3′) and reverse (5′-CAA-CAACGCACAGAATCTAC-3′) primers used were homologous with the DNA sequences upstream and downstream of the polyhedrin gene, respectively.

Production of the HPL(-lid) Mutant and the N-GPLRP2/C−HPL Chimera. These two mutants were expressed in insect cells as previously described (*19*) (see Figure 1).

Electrophoresis and Western Blotting Analysis. The total proteins present in the culture medium at various times after infection were analyzed by electrophoresis on 12% SDS−polyacrylamide gels in a Bio-Rad Mini Protean II cell (*24*). The gels were either stained with Coomassie brilliant blue or subjected to Western blot analysis.

The proteins were electrophoretically transferred from the gel onto a nitrocellulose membrane (BA 83 type, 0.45 μm) using the following transfer buffer: 20 mM Tris, 150 mM glycine pH 8.3 with 20% (v/v) methanol. The membrane was then washed with phosphate-buffered saline (PBS) (8 g/L NaCl, 0.1 g/L KH_2PO_4, 2.9 g/L Na_2HPO_4, 12 H_2O). To saturate the free sites, the membrane was incubated in a blocking solution containing 3% (w/v) skimmed milk dried in PBS for 1 h at room temperature. After three washes with PBS/Tween 20 (0.05% v/v), the membrane was incubated with purified anti-HPL antibodies (2 μg/mL) for 1 h at room temperature and then with secondary goat anti-rabbit (or mouse) immunoglobulins (Sigma) conjugated to alkaline phosphatase (dilution 1/2000) for 1 h at room temperature. The membrane was further washed three times with PBS/Tween 20 and twice with 0.1 M Tris-HCl buffer (pH 9.5) containing 0.1 M NaCl. The specific immunoreactivity was revealed with 0.1 M Tris-HCl buffer (pH 9.5) containing 0.1 M NaCl, 1 mM $MgCl_2$, 5 mM 5-bromo-4-

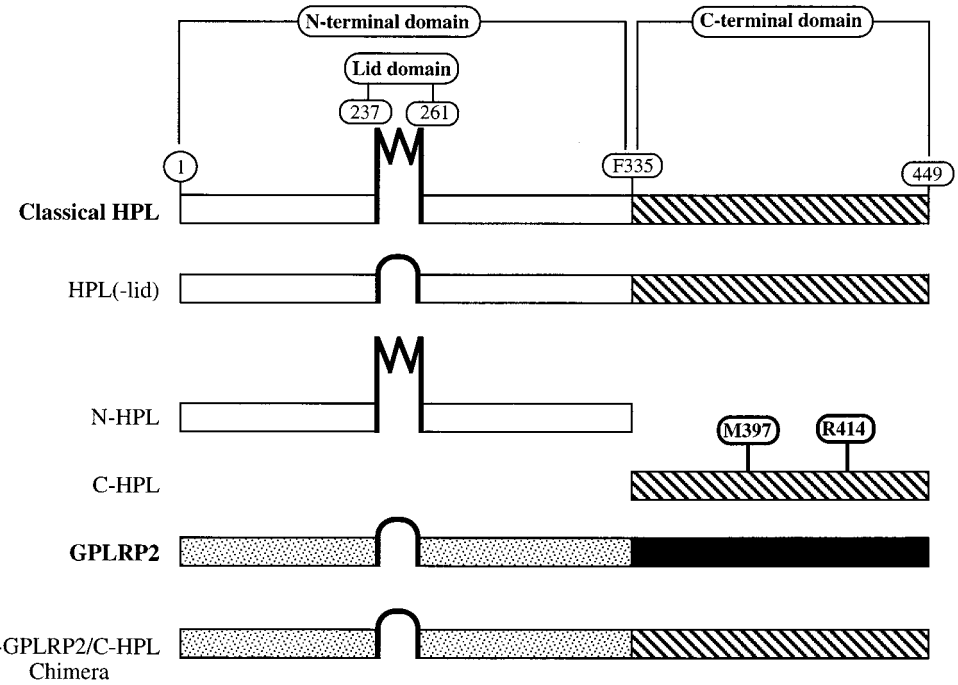

FIGURE 1: Diagram of the primary structure of HPL, GPLRP2, and the corresponding mutants. The HPL amino acid residues are numbered according to Winkler et al. (*14*). In HPL, the lid domain is the polypeptide region located between C237 and C261. Met 397 and Arg 414 are located within the C-terminal domain of HPL.

chloro-3-indolyl phosphate, and 3.5 mM nitroblue tetrazolium.

Anti-HPL Antibodies. Anti-HPL pAb and mAb's (numbered 81−23, 146−40, 315−25, and 320−24) were produced and characterized at our laboratory (*20*).

ELISA Tests. To test whether the mAb's (81−23, 315−25, and 320−24) recognized the colipase binding site on HPL, a double sandwich ELISA test was performed (*20*). A second ELISA test was performed in which microtiter plates were also coated with pure anti-HPL pAb (250 ng/well, captor antibody), and HPL was added (2.5 ng/well) to the PVC-coated pAb. The wells were emptied, washed, and dried by flicking. Fifty microliters of a pure porcine colipase solution in a 5-fold molar excess was added to each well.The lipase/colipase complex was subsequently incubated with the various mAb's (0.06−125 ng/well). The immunoreactivity of each mAb to HPL was detected with peroxidase-conjugated anti-mouse IgG antibody.

Dot Immunoassay. The interactions of the mAb's 81−23, 315−25, and 320−24 with native and SDS-treated HPL, as well as with the C-terminal domain alone, were studied by dot immunoassay (or dot-immunobinding assay) (*25*). Proteins were immobilized on nitrocellulose membrane. Once the proteins were fixed, we proceeded as described above in the case of the immunoblotting assay. The capacity of the C−HPL to bind colipase was also investigated. The colipase (20 μg) and the C−HPL (4 μg), used in the control assays, were immobilized separately on a poly(vinylidene difluoride) membrane (PVDF) and incubated in a blocking solution (see above). The C−HPL was then added (80 μg) and incubated for 2 h. The immunodetection was performed using anti-HPL pAb, and we proceeded as described above.

Preparation of C−HPL. C−HPL was obtained by performing limited chymotryptic cleavage on the native enzyme (*26*). Lipase (1.5−2 mg) was dissolved in 1 mL of 60 mM ammonium bicarbonate buffer, pH 8.5, and then incubated with TLCK-treated chymotrypsin (Sigma), (0.01 w/w) at 25 °C for 15 h. The proteolysis was stopped by adding phenyl methanesulfonyl fluoride at a final concentration of 2 mM. The proteolytic mixture was then loaded onto an Ultrogel AcA-54 column (1.5 cm × 200 cm), equilibrated, and eluted with 60 mM ammonium bicarbonate buffer, pH 8.5. The material eluted under the low molecular mass peak (a 14 kDa fragment corresponding to the HPL C-terminal domain) was pooled and concentrated using a Speed-Vac concentrator.

Cyanogen Bromide and Endoproteinase Arg-C Cleavage of the C−HPL. The 14 kDa C−HPL (5−10 nmol), which contains a single methionine residue (Met 397), was incubated with a solution of 70% formic acid containing a 180-fold molar excess of CNBr for 24 h at room temperature under nitrogen. The reaction was stopped by adding 6 volumes of cold water and then freeze-dried. The cleavage with the endoproteinase Arg-C (sequencing grade, Boehringer Mannheim) was performed in 10 mM Tris-HCl buffer, pH 7.6, containing 10 mM $CaCl_2$ with an enzyme-to-substrate ratio of 1:50 at 37 °C, for 18 h. The hydrolysis reaction was stopped with 1 mM 4-(2-aminoethyl)-benzenesulfonylfluorure, hydrochloride (Pefabloc-SC, Boehringer Mannheim). SDS-gel electrophoresis analysis of the cleaved domain was carried out on 10% Tris-Tricine gel (*27*).

After the electrophoresis, the peptides were transferred onto either a nitrocellulose or a PVDF membrane (0.45 μm) for Western blotting or N-terminal amino acid sequence analysis. Immunodetection was performed on nitrocellulose triplicates with mAb's 81−23, 315−25, and 320−24. Automated Edman degradation of the peptides transferred onto PVDF membrane was performed using an Applied Biosystems Model 473 A gas-phase sequencer. The resulting phenyl thiohyantoins were identified by performing HPLC on a C-18 Brownlee column (5 μm, 2.1 mm × 220 mm).

Measurement of Lipase and Esterase Activities. To test the effects of mAb's 81−23, 146−40, 315−25, and 320−

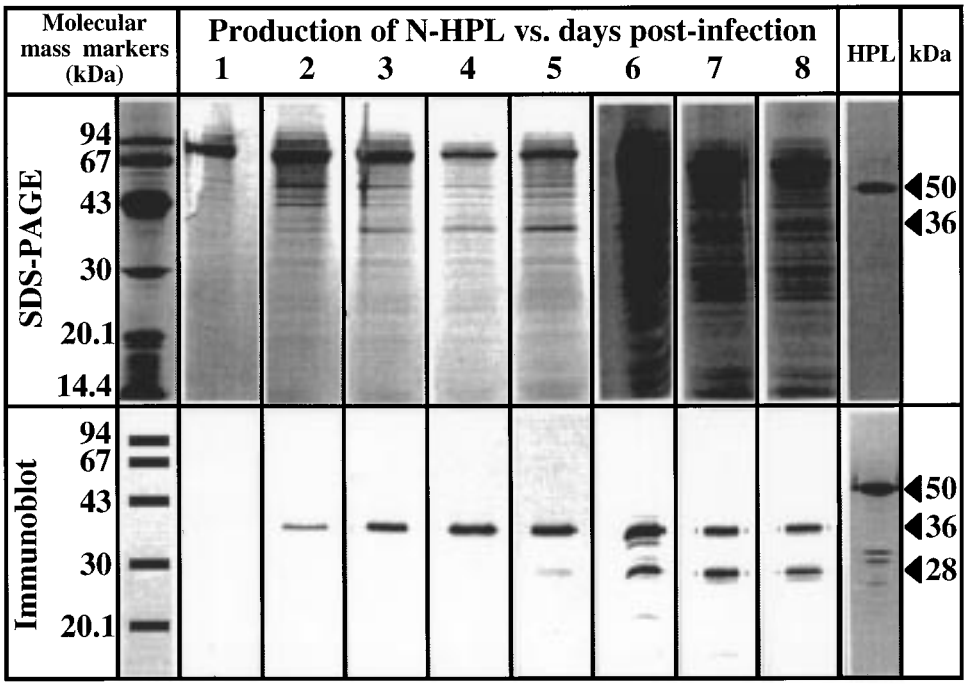

FIGURE 2: Time course of the production of N−HPL expressed in baculovirus-infected insect cells (Sf9) during the first 8 days after infection. Upper panel: SDS−PAGE (12%). Lower panel: Western blotting. The band of around 28 kDa corresponds to a partly degraded form of N−HPL. HPL (50 kDa) was used as the molecular mass standard.

24 on the lipolytic activity of HPL, three types of substrates were used: tripropionin (TC3), tributyrin (TC4), and trioctanoin (TC8). The mAb/HPL complexes were obtained by incubating each mAb in PBS for 1 h at 37 °C with HPL at an antibody/lipase molar ratio of 2. The residual activity of the HPL/mAb complexes was measured potentiometrically using a pH-stat (716 DMS Titrino, Metrohm). Assays on TC8 and TC4 were carried out under standard conditions (*20*, *28*), respectively. TC3 was used as the substrate for measuring the interfacial activation of HPL (*29*) and of the HPL/mAb complex. The TC3 solutions were systematically prepared by sonicating a given amount of TC3 in gum arabic 1% three times for 30 s. Before each assay, 5 mL of the solutions was added to 10 mL of pure water in the thermostated (37 °C) pH-stat vessel, at pH 7.0, in the presence of a 5-fold molar excess of colipase.

Surface Calculations on the HPL 3-D Structure. The surface area involved in the interaction between the N- and C-terminal domains of HPL and the area exposed to solvent within the C-terminal domain were calculated using the DSSP module from the Turbo-Frodo software program (*30*), on the basis of the coordinates of the open HPL/colipase complex (*17*) deposited in the Brookhaven Protein Data Bank (accession number 1LPA).

RESULTS

Expression of the N-Terminal Domain of HPL (N−HPL). A DNA fragment encoding the N-terminal domain of HPL was constructed by PCR and further cloned into a baculovirus transfer vector as described in Materials and Methods. A recombinant baculovirus was obtained after cotransfecting Sf9 insect cells with the transfer vector and the DNA of the wild-type AcMNPV baculovirus. The Sf9 cell cultures were then infected with the recombinant baculovirus with a multiplicity of infection of 10. A time-course experiment was performed for 8 days on N−HPL expression, in which samples of the culture medium were collected every day post-infection for SDS−PAGE and Western blotting analysis using pAb raised against native HPL (nHPL) (see Figure 2). A band at around 36 kDa, corresponding to the expected molecular mass of N−HPL (36.8 kDa calculated from the amino acid sequence), was detected 48 h after the infection and its intensity increased up to day five. On day five, degradation products appeared and the intensity of the 36 kDa band began to decrease simultanously with the emergence of several bands with lower molecular masses. This process reflects the proteolysis of N−HPL occurring after cell lysis on day four post-infection (*22*). In addition to the 36 kDa band, the main degradation product, which had a molecular mass of 28 kDa, was also recognized by anti-HPL pAb (see Figure 2).

Mapping of the HPL Structural Domains with the Four anti-HPL mAb's. The immunoreactivity of four anti-HPL mAb's and a pAb was studied using the N−HPL, HPL-(-lid), and N-GPLRP2/C−HPL chimera produced in a previous study (*19*), as well as nHPL, recombinant HPL (rHPL), and GPLRP2 as control proteins. As shown in Figure 3, the anti-HPL pAb reacted with all the lipase forms tested, including GPLRP2. In some cases, reactive bands with lower molecular masses occurred due to the presence of proteolytic fragments in the culture medium, as previously discussed in the case of N−HPL (see Figure 2). The mAb's exhibited a more selective pattern of recognition. First, none of the four mAb's cross-reacted with GPLRP2, which nevertheless shows 64% amino acid identity with HPL (*6*). Second, mAb 146−40 reacted with N−HPL and not with GPLRP2 or with N-GPLRP2/C−HPL chimera, which indicates that it specifically recognizes the N-terminal domain of HPL (Lys1-Phe335). Furthermore, the reactivity of this mAb with an HPL(-lid) indicates that the epitope recognized

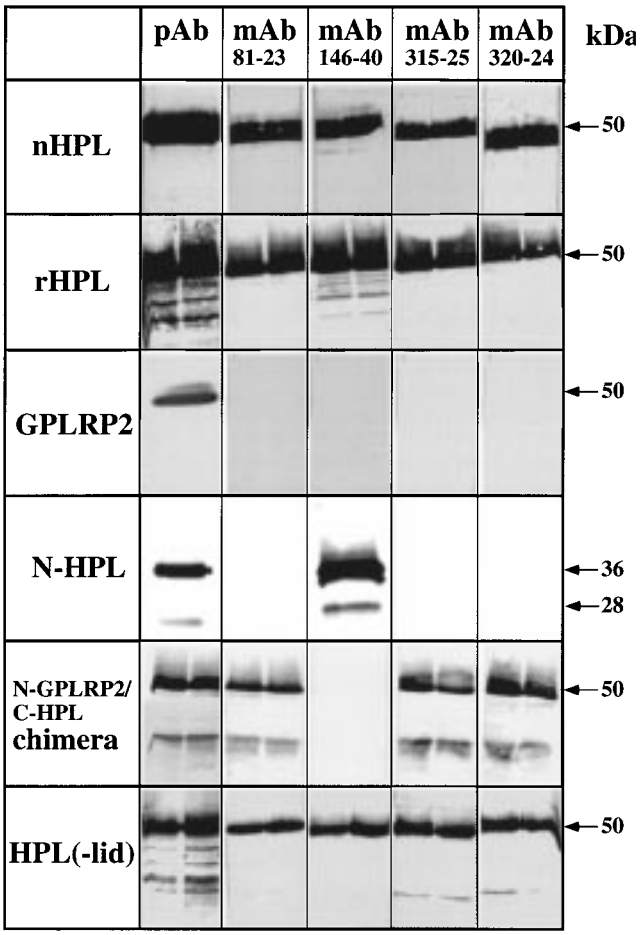

FIGURE 3: Immunoreactivity of anti-HPL pAb as well as mAb's 81−23, 146−40, 315−25, and 320−24 with native, recombinant, and mutant lipases. Native HPL (nHPL) was purified from human pancreatic juice (*42*). N−HPL samples were taken from the culture medium of insect cells (Sf9) 3 days post-infection. Recombinant HPL (rHPL) (*22*), GPLRP2 (*6*), N-GPLRP2/C−HPL chimera, and HPL(-lid) (*19*) were expressed at our laboratory and purified with an FPLC system. The multiple bands with lower molecular masses observed in some cases resulted from partial proteolysis.

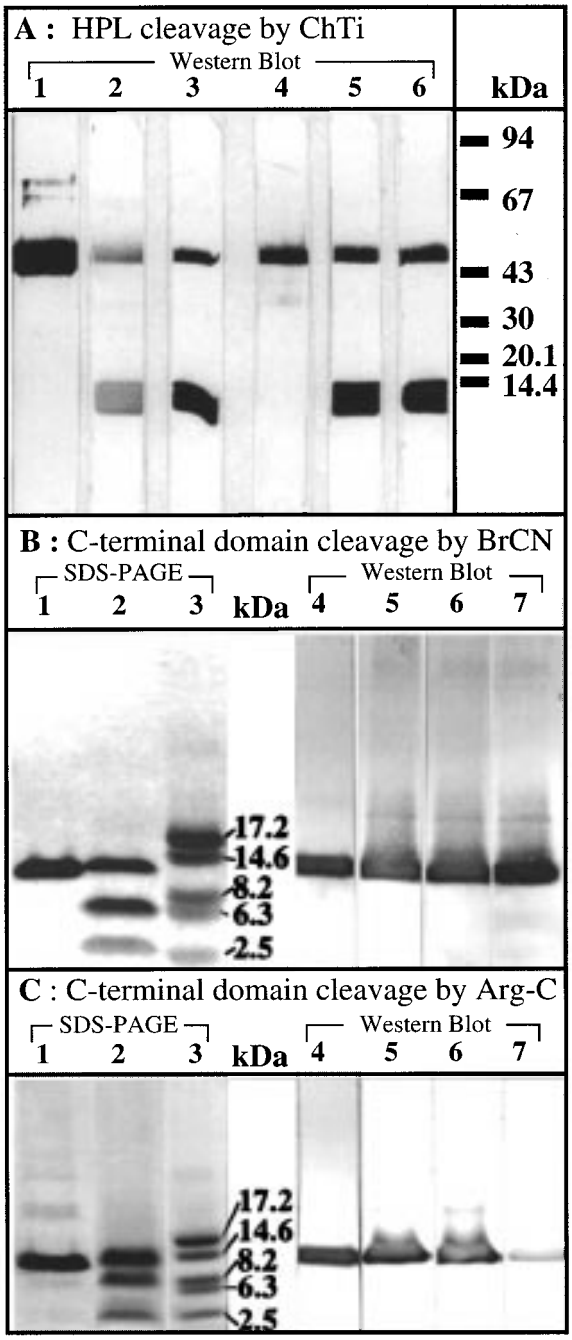

FIGURE 4: Western blot analysis of C−HPL fragments. (A) Reactivity with pAb and mAb's of the chymotryptic fragments of HPL. Lane 1 corresponds to native HPL revealed with pAb. Lanes 2−6 correspond to chymotrypsin-treated HPL revealed with pAb (lane 2) and mAb's 81−23 (lane 3), 146−40 (lane 4), 315−25 (lane 5), and 320−24 (lane 6). (B and C) SDS−PAGE (left side) and immunoreactivity (right side) of the C−HPL fragments produced by BrCN and endoproteinase Arg-C cleavages, respectively: lane 1, C−HPL; lane 2, fragments generated by BrCN (panel B) or Arg-C (panel C) cleavage; lane 3, Low molecular mass markers; lanes 4, 5, 6, and 7, incubation of the fragments generated by BrCN (panel B) or Arg-C (panel C) with anti-HPL pAb, mAb's 81−23, 315−25, and 320−24, respectively.

by mAb 146−40 is present in the core of the N−HPL and does not overlap with the lid domain (Cys 237-Cys 261). It has been reported that this antibody has no inhibitory effects on the activity of nHPL (*20*), which indicates that its epitope is not located in close proximity to the catalytic site. Third, mAb's 81−23, 315−25, and 320−24 cross-reacted with the N-GPLRP2/C−HPL chimera but not with GPLRP2 or with N−HPL, which suggests that the epitopes recognized by these three mAb's were probably located in the C-terminal domain of HPL (Ala336-Cys449). To confirm this hypothesis, we produced the C−HPL after its cleavage from the entire HPL using chymotrypsin (*26*). The proteolyzed fragments were then analyzed by performing Western blotting with the four mAb's. As shown in Figure 4 A, a fragment with a molecular mass of around 14 kDa not reacting with the mAb 146−40 (lane 4) was clearly revealed by mAb's 81−23 (lane 3), 315−25 (lane 5), and 320−24 (lane 6). On the basis of the N-terminal sequence analysis, this polypeptide was identified as the C-terminal domain of HPL (Ala336-Arg-Trp-Arg-Tyr-Lys-Val-Ser-Val-).

We did not determine any structural parameters of the C−HPL, but we checked that this domain alone was still able to bind to colipase. The binding of the C−HPL to colipase is mediated by at least 12 amino acid residues located close to each other within the 3-D structure but far apart along the primary structure (*31*). It seems unlikely that the colipase binding will be preserved when the C−HPL is unfolded. The binding of the C−HPL to colipase was investigated by dot immunoassay. The fact that the C−HPL

bound to the immobilized colipase supports the idea that the structure of the isolated C−HPL may show a similar pattern of folding to that which occurs in the case of the entire enzyme. Similar results have been obtained with the C-terminal domain of horse pancreatic lipase (*32*).

Epitope Mapping of the C−HPL. To further characterize these epitopes, we made use of the fact that a single methionine (Met 397) residue is present within the C-terminal domain. Two fragments resulting from the CNBr cleavage of the C−HPL were characterized by performing Western blotting (Figure 4B, lanes 4−7) as well as N-terminal amino acid sequence analysis. These two fragments (Ala336-Arg-Trp-Arg-Tyr... and Val398-Lys-Phe-Ile-Trp...) did not immunoreact with the three mAb's 81−23 (lane 5), 315−25 (lane 6), and 320−24 (lane 7), whereas a positive response was observed with the entire uncleaved C−HPL (lanes 5−7). These results suggest that the corresponding epitopes overlap the Met 397-Val 398 peptide bond.

In addition to undergoing CNBr cleavage, the C−HPL (Ala 336-Cys 449) was also subjected in parallel to endoproteinase Arg-C treatment. Four arginine residues are present in C−HPL and are located at positions 337, 339, 414, and 439 according to Winkler's system of numbering (*14*). The proteolytic cleavage of the purified C−HPL with endoproteinase Arg-C yielded two fragments. From their N-terminal sequence analysis (Tyr340-Lys-Val-Ser-Val and Val415-Gly-Ala-Ser-Lys), it was concluded that these two fragments result from the cleavage at Arg 414. Western blotting tests did not show the existence of any reactivity between these two fragments and the three mAb's 81−23 (Figure 4C, lane 5), 315−25 (lane 6), and 320−24 (lane 7). It was therefore concluded that the corresponding recognized epitopes probably overlap the Arg 414-Val 415 peptide bond.

Since it has been clearly established that colipase binds to the C-terminal domain of HPL in both the open and closed conformations, we investigated whether the epitopes recognized by mAb's 81−23, 315−25, and 320−24 were part of the colipase binding site. Two double sandwich ELISA tests were carried out in the presence and absence of colipase as described in the Materials and Methods section. These two ELISA tests gave identical titration curves (data not shown). There are two possible explanations for these results: (1) the epitope(s) recognized by these three mAb's is (are) distinct from the colipase binding site on HPL, or (2) the mAb's may dissociate the HPL/colipase complex due to HPL having a higher affinity for mAb ($K_d \approx 10^{-8}$ M) (*20*) than for colipase ($K_d \approx 10^{-6}$ M) (*33*). On the basis of the 3-D stucture of the HPL/colipase complex (Figure 5), Met 397 and Arg 414 are exposed at the surface of the HPL C-terminal domain and are located apart from the colipase binding site (*16, 31*). It therefore seems likely that colipase and the three mAb's investigated bind independently to the C-terminal domain of HPL.

Effects of SDS on the Epitope Recognition by mAb's 81−23, 315−25, and 320−24. The three-dimensional structure of HPL (Figure 5) shows that the Met 397 and Arg 414 are connected by a 16 amino acid long peptide but are nevertheless located close to each other within the 3-D structure of the C-terminal domain. This finding suggests that mAb's 81−23, 315−25, and 320−24 may recognize a conformational epitope. To test this hypothesis, we treated the purified C−HPL alone as well as HPL with variable amounts of SDS and tested the immunoreactivity by performing dot blotting experiments (Figure 6).

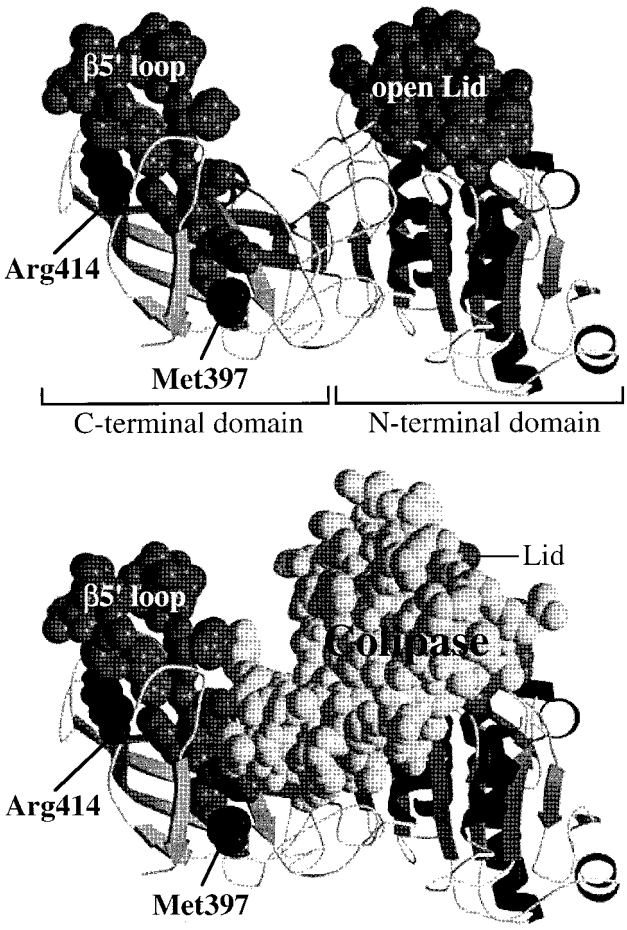

FIGURE 5: 3-D structure of HPL according to van Tilbeurgh et al. (*17*), with (lower panel) and without (upper panel) colipase. The open lid domain, the $\beta 5'$ loop, the colipase, Met 397, and Arg 414 are shown in CPK representation, whereas the rest of the HPL molecule is shown only by Cα tracing and is depicted as a ribbon model. The pictures were generated using the Molscript (*43*) and Raster3D (*44*) software programs.

In the case of the C−HPL, its immunoreactivity to each mAb was still detectable in the presence of 0.1% w/v SDS but decreased considerably at 1% w/v SDS and was completely nonexistent at 3% w/v SDS. Upon dialysis of the (3% w/v) SDS treated C−HPL, the immunoreactivity of the three mAb's was completely recovered. The reactivity of the three mAb's remained unchanged when intact HPL was used, even in the presence of 3% w/v SDS. The C−HPL as well as the intact HPL treated with 8 M urea in control experiments was no longer recognized by the three mAb's.

It can therefore be concluded that mAb's 81−23, 315−25, and 320−24 recognize a conformational epitope located at the C-terminal domain of HPL. In addition, the lack of immunoreactivity observed with the C−HPL in the presence of 3% w/v SDS, as opposed to the full immunoreactivity observed with intact HPL, strongly suggests that the N-terminal domain of HPL may prevent the denaturation by SDS of the C-terminal domain of HPL. Stabilizing interactions therefore occur between the two domains of HPL, which are not independent entities but which interact together via large surface areas (622 Å^2).

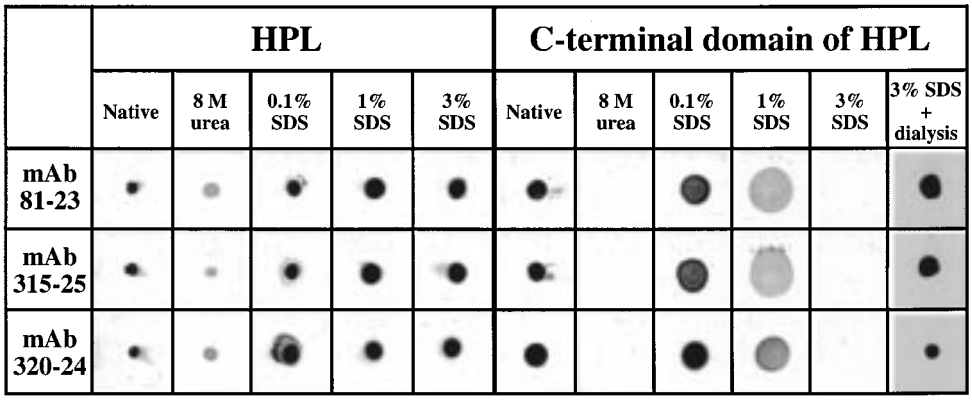

FIGURE 6: Dot immunoassay using mAb's 81−23, 315−25, and 320−24 against HPL or the C−HPL treated with either 8 M urea or increasing amounts of SDS. The amount of protein used in each test was 2 μg in the case of HPL and 2.5 μg in the case of C−HPL.

This epitope was not initially identified as a conformational one, since its immunoreactivity remained unchanged at the 0.1% w/v SDS concentration traditionally used for gel electrophoresis under so-called denaturating conditions (*24*). It was observed, however, in the present study that a 0.1% w/v concentration is not strong enough to denature the free C−HPL or that present in the intact HPL structure (Figure 6). It was also observed that the 3% w/v SDS concentration recorded in the sample buffer before protein loading in the SDS−PAGE procedure was still not sufficiently high to abolish the immunoreactivity of the conformational epitope within the intact HPL molecule. The immunoreactivity of the C−HPL was lost, however, at 3% w/v SDS and then recovered when the SDS concentration was further reduced upon dialysis. When performing Western blotting analysis to discriminate between conformational and sequential epitopes, it is therefore important to keep the following points in mind: first, the protein unfolding might not be complete at 3% w/v SDS; and second, the protein may be denatured during sample treatment at 3% w/v SDS and refolded within the separation gel at 0.1% w/v SDS.

Kinetic Characterization of the HPL/mAb Complexes. The anti-HPL mAb's 81−23, 315−25, and 320−24, or their Fab fragments, were previously found to inhibit the lipolytic activity measured on water-insoluble trioctanoin emulsions in the presence or absence of sodium taurodeoxycholate (NaTDC) and colipase (*20*). These data suggest that these mAb's probably mask an important site involved in the HPL interaction with the oil/water interface. Since HPL also displayed a significant level of esterase activity on tripropionin under its solubility limit (*29*), we checked whether the esterase activity on tripropionin monomers persisted in the case of the HPL/mAb complexes. For this purpose, the specific activities of the HPL/mAb's complexes were measured as a function of the tripropionin concentration (Figure 7). Although HPL clearly displayed interfacial activation above the tripropionin solubility level (12 mM), the specific activities of the three HPL/mAb's complexes always remained low and never exceeded the maximum value recorded with HPL below the solubility limit (275 ± 18 units/mg). The complexes were completely inactive toward pure trioctanoin, which is completely insoluble in water and where no free monomeric substrate is therefore available. The complexes displayed slight activity on tributyrin (55−96 units/mg), which has a low solubility (400 μM) in water. We furthermore checked that these changes

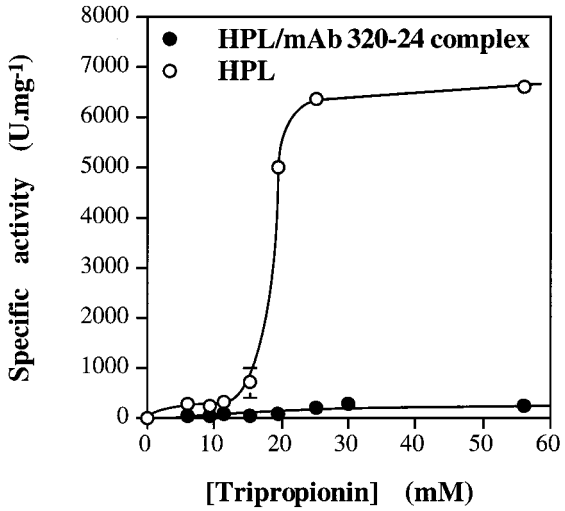

FIGURE 7: Specific activity versus tripropionin concentration of HPL (○) and the HPL/mAb 320−24 complex (●). In each assay, 1.4 μg of HPL or 10 μg of HPL bound to mAb 320−24 (2:1 molar ratio) was used. Further details about the interfacial activation test are given in Materials and Methods.

in the kinetic properties were specific to the mAb's recognizing the C-terminal domain of HPL. In fact, the HPL/mAb 146−40 complex consistently showed a similar lipase activity to that of HPL alone (Table 1).

In the culture medium in which N−HPL was produced, we measured the N−HPL activity on tripropionin and the N−HPL concentration by ELISA (*34*). These measurements yielded a specific activity of 105 units/mg, which is similar to the value obtained with the three HPL/mAb's complexes (Table 1).

DISCUSSION

The epitope mapping of HPL was reinvestigated in the present study using HPL mutants. In light of the results obtained here, the previously published data (*20*) had to be partly reinterpreted. The latter workers (*20*) reported that mAb's 81−23, 315−25, and 320−24 reacted with a 26 kDa chymotryptic fragment including the C-terminal domain and part of the N-terminal domain, whereas *no immunoreactivity* at all was observed here with C−HPL. The logical conclusion reached by the previous authors was that the epitopes recognized overlapped the hinge region. To investigate the reasons for the discrepancy between the present results and

Table 1: Specific Activities of HPL, HPL/mAb 81−23, HPL/mAb 315−25, HPL/mAb 320−24, N-HPL, and HPL/mAb 146−40 Complexes on TC3, TC4, and TC8 Substrates[a]

substrate	trioctanoin (67 mM)	tributyrin (114 mM)	tripropionin (9.2 mM)	tripropionin (56 mM)
HPL	9625 ± 185	9750 ± 264	275 ± 18	6600 ± 110
HPL/mAb 81−23	0	74 ± 11	65 ± 25	288 ± 9
HPL/mAb 315−25	0	96 ± 15	52[b] ± 12	257 ± 17
HPL/mAb 320−24	0	55 ± 9	40 ± 18	224 ± 21
N-HPL	0	0	48 ± 14	105 ± 38
HPL/mAb 146−40	8588 ± 220	10700 ± 320	184 ± 20	5985 ± 307

[a] The data (units/mg) given are means based on experiments performed in triplicate. [b] Similar values were obtained using various mAb/HPL molar ratios ranging from 2 to 6.

the previous ones (*20*), chymotryptic cleavage was performed on nHPL under controlled conditions and C−HPL was purified in order to study its immunoreactivity. The 14 kDa protein fragment obtained was clearly recognized by mAb's 81−23, 315−25, and 320−24 (Figure 4A). The previous results (*20*) are probably attributable to an incomplete chymotryptic treatment generating low amounts of the C−HPL (see Figure 4 in ref *20*). This possibility was supported by the fact that the 14 kDa band also showed a faint immunoreactivity with pAb (see Figure 4 in ref *20*).

Our results support the hypothesis that the three mAb's 81−23, 315−25, and 320−24 are directed against the same conformational epitope located within the C-terminal domain of HPL, in the vicinity of Met 397 and Arg 414 (Figure 5). Moreover, the competitive binding behavior of all three mAb's, or Fab fragments, with HPL and their dissociation constants and titration and immunoinactivation curves, is very similar (*20*).

Like all detergents, SDS can exist in aqueous solutions in the form of monomers and micelles. Its critical micellar concentration (CMC) is about 0.24% w/v. The results reported here show that the C−HPL unfolds only at SDS concentrations greater than the CMC value (1% and 3% w/v SDS). The denaturation of the C−HPL is apparently due to the presence of SDS micelles and thus to the presence of an interface. Recent studies at our laboratory have highlighted the importance of the C-terminal domain in the stability of pancreatic lipases at lipid/water interfaces (*19*). These studies showed that the interfacial denaturation of HPL depends on the structure of the C-terminal domain, and part of the C-terminal domain may therefore interact with the interface. These conclusions are supported by recent data (*35*). On the basis of the original 3-D structure at 3 Å resolution of the open form of the lipase/colipase complex in the presence of mixed bile salt/phospholipid micelles (*17*) as well as on low resolution (18 Å) neutron diffraction data, it was proposed (*35*) that a micelle of nonionic detergent tetraethylene glycol monooctyl ether may have interacted exclusively with colipase and the C-terminal domain of pancreatic lipase. These results are at variance with the data obtained in a recent study (*36*) at 2.46 Å resolution, in which several nonionic β−octylglucoside molecules in the lipase/colipase complex inhibited by C11 alkyl phosphonate were clearly found to be located along the extended hydrophobic plateau consisting of the lid domain, the β9 loop, and the hydrophobic tips of colipase, thus mimicking the interaction between the lipase/colipase complex and the lipid interface. Furthermore, it was concluded (*35*) that the micelle and substrate binding by the lipase/colipase complex involves various regions of the enzyme and that the activation of pancreatic lipase is not an interfacial phenomenon. Here we clearly illustrated the interfacial activation phenomenon which occurs in the absence of detergent micelles upon studying the kinetic properties of the HPL/mAb's complexes, which continued to show a low level of activity on soluble substrate (tripropionin and tributyrin monomers), whereas their lipase activities were lost on insoluble substrate (trioctanoin) (Table 1). The finding that C−HPL plays an important role in the lipase activity is in agreement with the preliminary characterization of the N−HPL mutant, devoid of the C-terminal domain. N−HPL was found to have a similar specific activity on tripropionin to that of the three HPL/mAb's complexes and to be inactive toward trioctanoin (Table 1). We can suggest one tentative hypothesis, however, to explain our experimental data: in the presence of mAb, the lid cannot interact with the colipase, so that the closed pancreatic lipase conformation, that is, low enzymatic activity on monomeric substrate, will be favored. The absence of lid opening could also explain the low catalytic activity on monomers (48 units/mg) of the recombinant N-terminal domain of HPL. It will be necessary, however, to purify this mutant in order to be able to carry out more detailed kinetic studies.

The results obtained in the present study suggest that an exposed loop of the C-terminal domain of pancreatic lipase may be involved in the interaction with the interface. This loop, named $\beta5'$ according to Winkler's system of numbering (*14*), is located between Met 397 and Arg 414 and is probably part of the conformational epitope recognized by mAb's 81−23, 315−25, and 320−24. The Met 397-Arg 414 stretch is highly accessible to solvent in HPL (1089 Å^2), and its accessibility remains almost unchanged in the HPL/colipase complex (996 Å^2), as can be seen from Figure 5. Only three residues in this stretch are partly masked by colipase: Lys 399 (−40 Å^2), Ile 401 (−14 Å^2), and Tyr 403 (−39 Å^2). These data support the hypothesis that colipase and the three mAb's (81−23, 315−25, and 320−24) may recognize distinct parts of the C-terminal domain of HPL. The $\beta5'$ loop (residues 405−414) exhibits a large accessible surface area (877 Å^2), which is significantly hydrophobic (H = 488 Å^2). Charged (C) and semi-polar (S) residues have accessible surfaces areas of C = 105 Å^2 and S = 284 Å^2, respectively. Consequently, the hydrophilic/lipophilic balance (HLB = $(C + S)/H$) is equal to 0.8 and is identical to that of the open lid domain (*18*). As shown in the 3-D structure of HPL (Figure 5), the hydrophobic $\beta5'$ loop, together with the open lid domain, might well contribute to the occurrence of lipase interactions with an interface. It

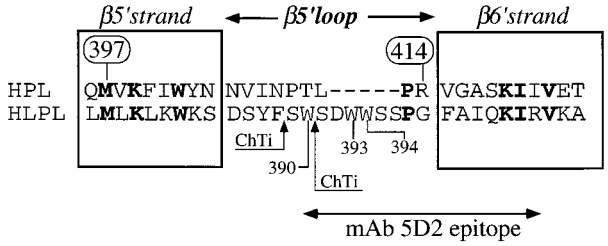

FIGURE 8: Amino acid sequence alignment of HPL and human LPL (HLPL) in the region of the $\beta 5'$ loop. HPL amino acid residues and secondary structures are numbered according to Winkler et al. (*14*). Arrows indicate the chymotrypsin cleavage site observed in bovine LPL (*40*). The mAb 5D2 epitope in HLPL shown is that determined in refs *37* and *39*.

can also be seen from Figure 5 that the potential contribution of the $\beta 5'$ loop to the interfacial binding is not masked in the presence of colipase.

Similar studies on lipoprotein lipase (LPL) have suggested that a putative exposed loop in the C-terminal domain of LPL may play an important role (*37*−*39*). Upon performing sequence alignment, this loop was found to be located at the same position as the $\beta 5'$ loop of HPL (residues 405−414), but it contains a large insertion including three tryptophan residues (Figure 8). Experiments of several kinds have been carried out to modify this loop in LPL: immunoreaction with a mAb (5D2) (*37*−*39*), proteolytic cleavage by chymotrypsin (*40*), and site-directed mutagenesis of Trp 390, Trp 393, and Trp 394 in human LPL (*39*, *41*). All these approaches resulted in a decrease in the activity against long-chain triglyceride emulsions and chylomicron (which are completely water-insoluble substrates), whereas the esterase activity on soluble substrates such as tributyrin was preserved. It was concluded that the $\beta 5'$ loop of LPL contributes to the binding of LPL to lipid/water interfaces.

These results demonstrate for the first time that the C-terminal domain of pancreatic lipase not only is essential to colipase binding but also may play an important role in the interfacial binding of pancreatic lipase, together with the lid domain (*17*) and the $\beta 9$ loop (*18*). Blocking the $\beta 5'$ loop with a mAb therefore abolishes the interfacial activity of classical pancreatic lipases.

ACKNOWLEDGMENT

This research was carried out in the framework of the EC Biotech-G Lipase projects (BIO2-CT94-3041 and BIO2-CT94-3013). Our thanks are due to Daniel Campese (CNRS Marseille) for performing the N-terminal sequence analysis and Dr. Jessica Blanc for revising the English. We particularly acknowledge the help of Drs. Christian Cambillau, Yves Bourne, and Alain Roussel (AFMB-CNRS Marseille) with the image processing of Figure 5. We are grateful to Dr. Laurence de La Fournière (UPR 9025-CNRS Marseille) for providing the mAb's.

REFERENCES

1. Verger, R. (1984) in *Lipases* (Borgström, B., and Brockman, H. L., Eds.) pp 83−149, Elsevier, Amsterdam, The Netherlands.
2. De Caro, J., Boudouard, M., Bonicel, J., Guidoni, A., Desnuelle, P., and Rovery, M. (1981) *Biochim. Biophys. Acta 671*, 129−138.
3. Lowe, M. E., Rosenblum, J. L., and Strauss, A. W. (1989) *J. Biol. Chem. 264*, 20042−20048.
4. Giller, T., Buchwald, P., Blum-Kaelin, D., and Hunziker, W. (1992) *J. Biol. Chem. 267*, 16509−16516.
5. Kerfelec, B., La Forge, K. S., Puigserver, A., and Scheele, G. (1986) *Pancreas 1*, 430−437.
6. Hjorth, A., Carrière, F., Cudrey, C., Wöldike, H., Boel, E., Lawson, D. M., Ferrato, F., Cambillau, C., Dodson, G. G., Thim, L., and Verger, R. (1993) *Biochemistry 32*, 4702−4707.
7. Carrière, F., Thirstrup, K., Hjorth, S., and Boel, E. (1994) *FEBS Lett. 338*, 63−68.
8. Wicker-Planquart, C., and Puigserver, A. (1992) *FEBS Lett. 296*, 61−66.
9. Payne, M., Sims, H., Jennens, M., and Lowe, M. (1994) *Am. J. Physiol. 266*, G914−G921.
10. Thirstrup, K., Verger, R., and Carrière, F. (1994) *Biochemistry 33*, 2748−2756.
11. Thirstrup, K., Carrière, F., Hjorth, S. A., Rasmussen, P. B., Nielsen, P. F., Ladefoged, C., Thim, L., and Boel, E. (1995) *Eur. J. Biochem. 227*, 186−193.
12. Aleman-Gomez, J. A., Colwell, N. S., Sasser, T., and Kumar, V. B. (1992) *Biochem. Biophys. Res. Commun. 188*, 964−971.
13. Jennens, M. L., and Lowe, M. E. (1995) *J. Lipid Res. 36*, 1029−1036.
14. Winkler, F. K., d'Arcy, A., and Hunziker, W. (1990) *Nature 343*, 771−774.
15. Ollis, D. L., Cheah, E., Cygler, M., Dijkstra, B., Frolow, F., Franken, S. M., Harel, M., Remington, S. J., Silman, I., Schrag, J., Sussman, J. L., Verschueren, K. H. G., and Goldman, A. (1992) *Protein Eng. 5*, 197−211.
16. van Tilbeurgh, H., Sarda, L., Verger, R., and Cambillau, C. (1992) *Nature 359*, 159−162.
17. van Tilbeurgh, H., Egloff, M.-P., Martinez, C., Rugani, N., Verger, R., and Cambillau, C. (1993) *Nature 362*, 814−820.
18. Withers-Martinez, C., Carrière, F., Verger, R., Bourgeois, D., and Cambillau, C. (1996) *Structure 4*, 1363−1374.
19. Carrière, F., Thirstrup, K., Hjorth, S., Ferrato, F., Nielsen, P. F., Withers-Martinez, C., Cambillau, C., Boel, E., Thim, L., and Verger, R. (1997) *Biochemistry 36*, 239−248.
20. Aoubala, M., de La Fournière, L., Douchet, I., Abousalham, A., Daniel, C., Hirn, M., Gargouri, Y., Verger, R., and De Caro, A. (1995) *J. Biol. Chem. 270*, 3932−3937.
21. Sambrook, J., Fritsch, E. F., and Maniatis, T. (1989) *Molecular Cloning: a laboratory manual*, 2nd ed., Cold Spring Harbor Laboratory Press, New York.
22. Thirstrup, K., Carrière, F., Hjorth, S., Rasmussen, P. B., Wöldike, H., Nielsen, P. F., and Thim, L. (1993) *FEBS Lett. 327*, 79−84.
23. Marsh, J. L., Erfle, M., and Wykes, E. J. (1984) *Gene 32*, 481−485.
24. Laemmli, U. K. (1970) *Nature 227*, 680−685.
25. Hawkes, R., Niday, E., and Gardon, J. (1982) *Anal. Biochem. 119*, 142−147.
26. Bousset-Risso, M., Bonicel, J., and Rovery, M. (1985) *FEBS Lett. 182*, 323−326.
27. Schägger, H., and von Jagow, G. (1987) *Anal. Biochem. 166*, 368−379.
28. Erlanson, C., and Borgström, B. (1970) *Scand. J. Gastroenterol. 5*, 293−295.
29. Ferrato, F., Carrière, F., Sarda, L., and Verger, R. (1997) in *Methods in Enzymology*. (Dennis, E., and Rubin, B., Eds.) pp 327−347, Academic Press, New York.
30. Roussel, A., and Cambillau, C. (1991) in *Silicon Graphics Geometry Partners Directory* (Graphics, S., Eds.) pp 86, Silicon Graphics, Mountain View, CA.
31. Egloff, M.-P., Sarda, L., Verger, R., Cambillau, C., and van Tilbeurgh, H. (1995) *Protein Sci. 4*, 44−57.
32. Ayvazian, L., Crenon, I., Granon, S., Chapus, C., and Kerfelec, B. (1996) *Protein Eng. 9*, 707−711.
33. Donner, J., Spink, C. H., Borgström, B., and Sjöholm, I. (1976) *Biochemistry 15*, 5413−5417.
34. De Caro, A., Bezzine, S., Lopez, V., Aoubala, M., Daniel, C., Verger, R., and Carrière, F. (1998) in *Methods in Molecular*

Biology (Doolittle, M. H., and Reue, K., Eds.) Academic Press, New York (in press).
35. Hermoso, J., Pignol, D., Penel, S., Roth, M., Chapus, C., and Fontecilla-Camps, J. C. (1997) *EMBO J. 16*, 5531−5536.
36. Egloff, M.-P., Marguet, F., Buono, G., Verger, R., Cambillau, C., and van Tilbeurgh, H. (1995) *Biochemistry 34*, 2751−2762.
37. Liu, M. S., Ma, Y., Hayden, M. R., and Brunzell, J. D. (1992) *Biochim. Biophys. Acta 1128*, 113−115.
38. Wong, H., Davis, R. C., Thuren, T., Goers, J. W., Nikazy, J., Waite, M., and Schotz, M. C. (1994) *J. Biol. Chem. 269*, 10319−10323.
39. Lookene, A., Groot, N. B., Kastelein, J. J. P., Olivecrona, G., and Bruin, T. (1997) *J. Biol. Chem. 272*, 766−772.
40. Lookene, A., and Bengtsson-Olivecrona, G. (1993) *Eur. J. Biochem. 213*, 185−194.
41. Williams, S. E., Inoue, I., Tran, H., Fry, G. L., Pladet, M. W., Iverius, P. H., Lalouel, J. M., Chappell, D. A., and Strickland, D. K. (1994) *J. Biol. Chem. 269*, 8653−8658.
42. De Caro, A., Figarella, C., Amic, J., Michel, R., and Guy, O. (1977) *Biochim. Biophys. Acta 490*, 411−419.
43. Kraulis, P. (1991) *J. Appl. Crystallogr. 24*, 946−950.
44. Merrit, E. A., and Murphy, M. E. P. (1994) *Acta Crystallogr. D50*, 869−873.

BI973136R